LA-UR-01-3794
Approved for public release;
distribution is unlimited.

Title: **EXPERIMENTAL HEAT LEAK MEASUREMENTS ON THE APT 210 KW CW RF POWER COUPLER**

Author(s): J.A. Waynert, P.E. Blumenfeld, F.C. Prenger, J.P. Kelley, S.A. Currie, J.A. Stewart

Submitted to:

EXPERIMENTAL HEAT LEAK MEASUREMENTS ON THE APT 210 KW CW RF POWER COUPLER

J.A. Waynert, P.E. Blumenfeld[a], F.C. Prenger, J.P. Kelley, S.A. Currie, J.A. Stewart

Los Alamos National Laboratory
Los Alamos, NM 87544 USA

[a]Conductus, Inc
Sunnyvale, CA 94085 USA

ABSTRACT

A cryogenic test rig was designed and fabricated to measure the heat leak from room temperature to 2 K from the Accelerator Production of Tritium (APT) 700 MHz, 210 kW continuous wave (CW) co-axial power coupler (PC). The outer conductor of the PC is stainless steel with 15 μm copper film on the inside. The copper inner conductor operates at room temperature and contributes considerable infra-red radiation heat load to 2 K. Two thermal intercept heat exchangers cooled by supercritical helium are incorporated into the outer conductor to reduce the heat conducted to the lowest temperatures. A brief description of the experimental apparatus is presented. A comparison of the experimental measurements and the predictions of a detailed thermal model is given. There is also a discussion of anomalous behavior observed in the thermal intercepts, and fluctuations in the helium coolant properties.

INTRODUCTION

The original baseline APT (Accelerator Production of Tritium) linac design transmits 210 kW CW RF power at 700 MHz to the superconducting niobium accelerating cavities. The power coupler (PC) is a co-axial design with RF power transmitted in the annular region between two concentric cylinders. Thermally, the PC links room temperature to the 2 K operating temperature of the cavities within the cryomodule. Within the cryomodule, only the cavities represent a higher heat load on the cryogenic system [1]. Because of the large number of PCs needed (of the order of 100), and the large impact of their cooling on the cryogenic and distribution systems, and the cryomodule design, a detailed thermal

model was developed to explore a variety of design configurations, cooling approaches, and to optimize the total system refrigeration input power.

The details of the thermal model are presented in [2]. Ultimately, a PC design with two thermal intercepts was chosen to optimize the manufacturability of the cryomodule and the interface to the cryo-plant. An apparatus called the Cryogenic Test Rig (CTR) was designed and fabricated to verify the PC heat leaks, determine the effectiveness of the thermal intercept heat exchangers, and to compare measured temperatures with the thermal model temperature distribution predictions.

In what follows, there is a brief description of the thermal model, followed by a description of the experimental apparatus, the measurements taken, a presentation of some of the results and a comparison to the thermal model predictions. In addition, there is a discussion of sensitivity analysis. Finally, some observations of supercritical helium coolant flow oscillations are presented.

THERMAL MODEL DESCRIPTION

Figure 1 shows a schematic view of the PC as modeled. The left end of the PC operates at room temperature, while the right end is normally attached to the beam tube, which connects to the helium vessel at 2 K. There are two thermal intercept heat exchangers used to intercept and remove heat that would normally be conducted to 2 K. The high temperature heat exchanger (hex) would normally operate around 30 K and the low temperature hex around 7 K. The low temperature heat exchanger also ensures that the niobium nipple remains superconducting.

The thermal model is axisymmetric, one-dimensional, and uses a finite difference approximation. There are over 200 nodes. Temperature dependent properties are used for the thermal conductivities of copper (RRR = 50), 304 L stainless steel and niobium (RRR = 40 as measured experimentally), RF resistivity (RRR = 2, for 750 MHz), specific heat, thermal conductivity, Prandtl number, viscosity, and enthalpy of the helium gas coolant. Infrared radiation heating is calculated assuming gray body, diffuse scattering through a CAD based program called RadCAD [3]. SINDA [4] is used for the thermal analyzer.

The heat transfer mechanisms considered for the inner conductor are: conduction through copper (RRR=50); radiation (gray body, diffuse, copper emissivity ranging from

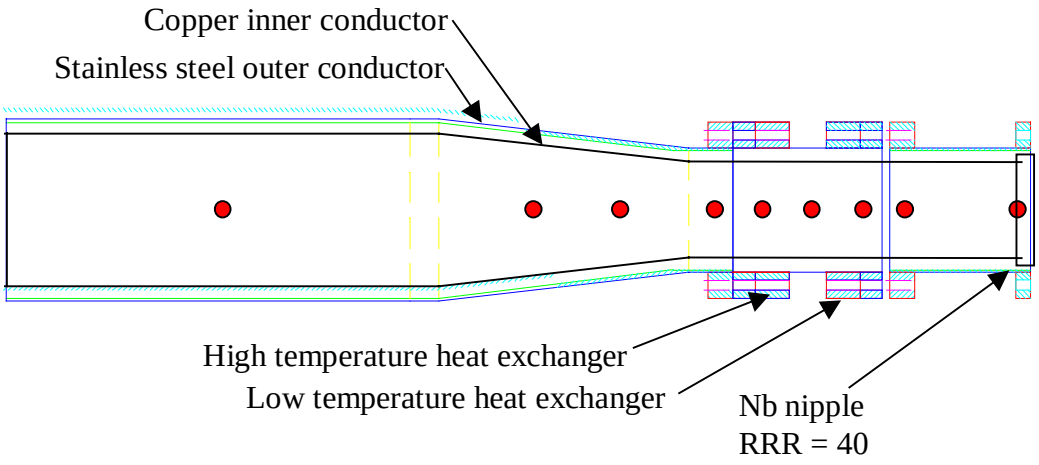

FIGURE 1. Schematic of the PC. Total length is about 1 m. The 304 L stainless steel outer conductor inner diameter is 152.4 mm at the 300 K end and tapers to 100 mm at the 2 K end. The copper inner conductor has a similar taper going from 66.7 mm outer diameter to 43.5 mm. There is a 15 μm copper film on the inside of the outer conductor. Dots on centerline are the locations of silicon diode thermometers.

0.05 to 0.1); RF heating (constant current or distributed power dissipation results from MAFIA[5]); and internal forced convection cooling by helium gas.

The outer conductor heat transfer mechanisms considered are: conduction through stainless steel (SS) (304L) and copper plating (thermal conductivity corresponding to RRR ranging from 5 to 50); radiation (gray body diffuse with SS emissivity ranging from 0.08 to 0.3 and Nb ranging from 0.1 to 0.3); and forced convection cooling in the thermal intercept heat exchangers using supercritical helium.

EXPERIMENTAL APPARATUS AND TEST PLAN

Figure 2 shows a picture of the PC test article hanging from the CTR top plate which is then inserted in a large vacuum vessel whose inner wall facing the PC is cooled with liquid helium. One end of the PC must be maintained at 300 K, the other end at 4 K. The CTR was originally designed to maintain the PC cold end at 2 K, but finite element analysis indicated that the temperature rose from the 2 K helium vessel through the beam tube to the connection to the PC to reach about 4 K.

The temperature of the supercritical helium supplied by a Koch 1610 liquefier to either hex can be raised to provide the appropriate inlet conditions using the heaters shown in Fig. 2. Inlet and outlet temperatures, the mass flow rate, the corresponding pressure drop, and the absolute pressure can be measured for both hex's. Thus, the heat load absorbed by the helium, q can be determined from $q = \dot{m} * \Delta h$ where $\dot{m}$ is the mass flow rate in kg/s, and Δh is the change in enthalpy in J/kg. The enthalpy is a strong function of pressure and temperature in this operating range [6]. The heat load at 4 K can be determined by the boil-off rate of the liquid helium in the toroidal dewar attached to the cold end of the Nb nipple via a copper plate shown in Figure 2. Figure 1 shows the location of a series of

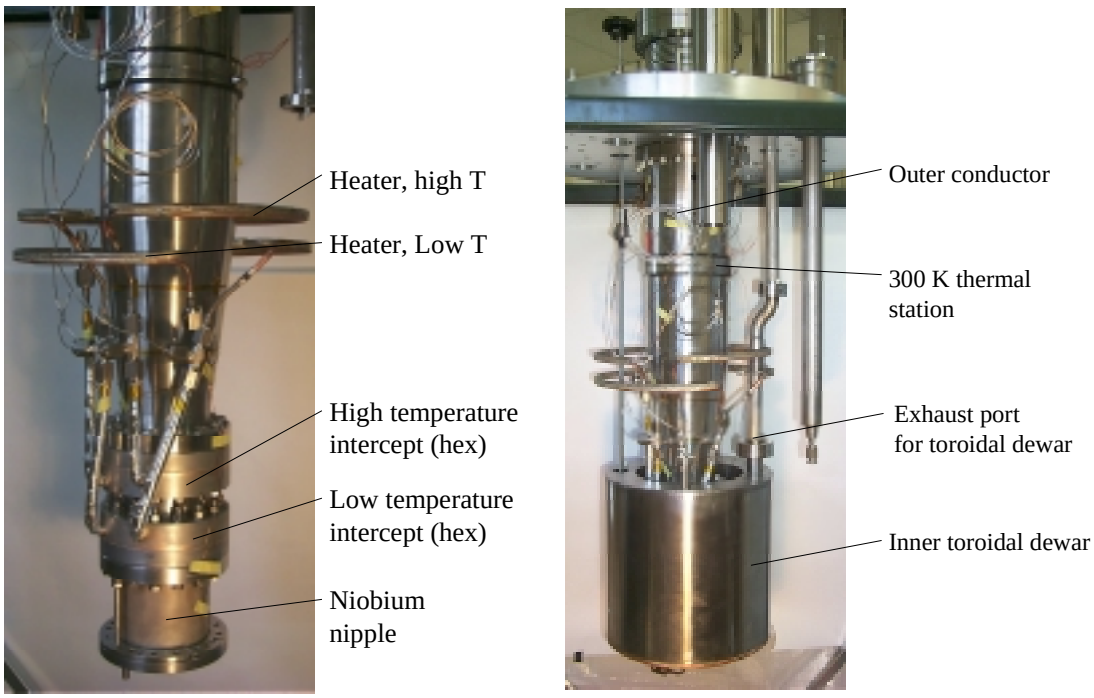

FIGURE 2. PC test article. Figure on left shows Nb nipple attached to SS nipple, which has two thermal intercept heat exchangers to remove heat being conducted from room temperature. Figure on right shows toroidal dewar attached to bottom of Nb nipple to measure heat leak to the lowest temperature, typically 4 K.

thermometers on the outer conductor whose measurements can be compared to the predicted temperature distribution. In one of the later experiments, resistive heater wire was bonded to the outer conductor surface using GE 7031 varnish. A current passed through the wire heated the PC conductor to simulate RF heating.

The first experiment used an outer conductor with no copper plating inside. The inner conductor (see Fig 1) was replaced with a series of parallel sheets of MLI (multi-layer insulation) mounted perpendicular to the axis of a G-10 thermally insulating rod. This MLI tree would minimize the infrared (IR) heat load to the inside of the outer conductor, thus eliminating the need to know the emissivities of the various materials. The second experiment was a repeat of the first experiment, except that the MLI tree was replaced with the actual inner conductor. The difference in heat loads between experiments 1 and 2 was due to the IR heat load. It was envisioned that the emissivities of the materials could then be determined from the change in temperature distributions on the outer conductor and from the change in heat loads. In the last experiment, the outer conductor was replaced with one having the appropriate electroplated copper on the inside. In addition, heater wires were attached to the outer conductor to be able to simulate the RF joule heating load when the PC is carrying 210 kW of traveling wave power.

The experimental data acquired were: temperature distribution on the outer conductor; temperatures of the helium in the CTR outer and toroidal dewars; the temperature of the copper plate (which is thermally linked to the toroidal dewar) to which the Nb nipple is attached; temperatures of the inlets and outlets to both hex's; absolute pressure at the inlet to the low T hex; pressure drop across each PC hex (generally found to be in the noise of the absolute pressure variation); mass flow rate to the hex's; mass flow rate of the boil-off helium from the toroidal dewar; liquid levels of the inner toroidal and outer CTR dewars; and heater power to the heater wire wrapped on the outer conductor to simulate RF heating.

RESULTS AND COMPARISON TO THERMAL MODEL

During the first experiment, there was difficulty interfacing to the supercritical helium for the intercept hex's. Thus, measurements were taken with no flow to these two hex's. This greatly increased the heat load to 4 K, which could still be measured, as well as the temperature distribution on the outer conductor. In comparing the measured and predicted temperature distributions, there are two unknown parameters: the contact conductances at the two conflat flanges shown in Fig 1. Figure 3 shows the comparison between the measured (squares) and the predicted (smooth line) temperature distributions. Choosing a contact conductance at the stainless steel interface of 1.4 W/K and 0.27 W/K at the Nb interface, results in very good agreement between the two temperature distributions. The conductance values were found to be in rough agreement with other experiments [7,8]. The measured and predicted heat loads at 4 K are 8.0 W and 6.8 W respectively. The difference is less than 18%, which is excellent agreement for these types of measurements.

For the second series of experiments, the MLI tree was replaced with the copper inner conductor and the coolant flow to the thermal intercept hex's was established. A number of interesting anomalies were observed in the hex performance, but space limitations prevent their discussion here. (For more information, see [9]).

Without the copper plating on the inside of the outer conductor, there are three materials; SS, Nb, and Cu that exchange IR radiation in a closed system. The best fit of the measured temperatures and the heat leak at 4 K to the SINDA model were obtained using emissivities for SS, Nb, and Cu of 0.08, 0.1 and 0.1 respectively based on [10,11]. The measured and predicted 4 K heat loads, 0.88 and 0.83 W, respectively, were very close.

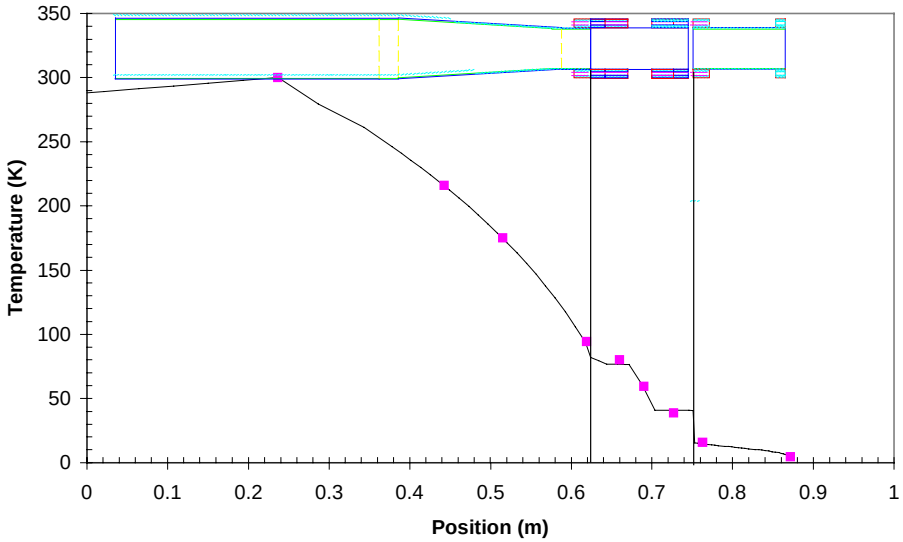

FIGURE 3. Comparison of thermal model predictions, solid line, to the measured temperature distribution, square dots for experiment 1 with no inner conductor and the thermal intercepts not being used. The outer conductor is shown to clarify the location of the thermometers.

Generally, the measured and SINDA-model-predicted 4 K heat leaks were within about 25% of each other and the temperatures above 100 K agreed to within 5 K. Lower temperature agreement was generally within 1 K.

In the third series of experiments on the PC, copper plating was added to the inner diameter of the outer conductor and resistive heater wire was added to simulate RF joule heating. With no RF simulated heating, the temperature measurements on the tapered portion of the outer conductor, where the temperature is generally greater than 50 K, were about 20 K below the model predictions. This difference is much greater than the expected error in the calibrated silicon diode thermometers. Hence, it was assumed that the thermal model input required some changes.

In evaluating various input changes to the thermal model, it is possible to 'disconnect' the low temperature portion, temperature < 20 K, from the upper temperature portion by connecting a fixed temperature boundary node with a high conductance to the wall temperature node of the higher temperature thermal intercept heat exchanger. Because the measured temperatures are lower than the predicted temperatures, the model appears to be predicting more 'generation like' heating in the outer conductor. A variety of changes to the model input were investigated including: emissivity of the materials; copper plating thickness; copper RRR; thickness of the stainless steel (SS) outer conductor; linearly tapering the SS wall thickness; tapering the copper plating thickness; and using a constant thermal conductivity for the SS. It was found that better agreement could be made by lowering the conductance values in the high temperature range and increasing the conductance in the lower temperature (still above 20 K) range.

The best agreement between measured and calculated temperatures came from choosing a constant thermal conductivity of 12 W/m-K for the SS. (The thermal conductivity of SS varies roughly as the square root of the temperature, varying from 15 W/m-K at 300 K to about 0.2 W/m-K at 4 K.) No physical reason could justify behavior independent of the temperature, since the thermal conductivity of most austenitic stainless steels fall within about ± 10% of each other at a given temperature [12]. The next best fit of the data to the model results, $T_{calc} - T_{measured} \leq 5$ K, was obtained by using a copper film RRR = 200. The copper film was electrolytically deposited, and coupons had a measured RRR = 4. Because the films for the CTR experiments were not heat treated or vacuum baked, the RRR was not expected to change.

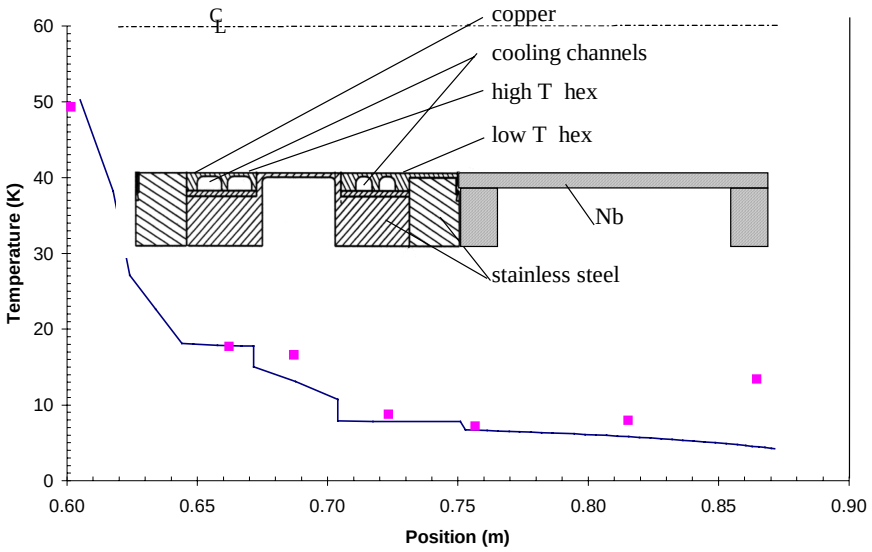

FIGURE 4. The measured (squares) and predicted (continuous line) temperature distribution in the low temperature portion of the outer conductor. The inset shows a cross-sectional view of that portion of the outer conductor with the thermal intercept heat exchangers and niobium nipple. Coolant mass flow rate was 0.2 g/s at a pressure of 9.8 bar.

Unfortunately, we did not measure the RRR of the copper on the actual outer conductor

The low temperature portion of the thermal model, for temperatures less than 50 K, corresponds to the spool piece with the two thermal intercept heat exchangers and the niobium nipple. Figure 4 compares the measured and predicted temperature distributions. The inset in the figure shows a cross-sectional view of that portion of the outer conductor with the two thermal intercept heat exchangers and their coolant channels for the supercritical helium. For the case shown, the upper temperature hex has a wall temperature of about 20 K and the lower temperature hex of about 8 K. The thermometers at positions 0.82 and 0.86 indicate a temperature gradient which would conduct heat away from the interface to the toroidal dewar to which the niobium nipple is attached. This is inconsistent with the observed 1 W boiloff heat load in the toroidal dewar. Hence, it was assumed that these two thermometers were not reading correctly. The contact conductances from the knife edge at the left end of the figure and between the SS and the niobium nipple were assumed to be the same as determined in the first experiment; at least, comparison to later data could not justify changing the conductance values. The contact conductance between the niobium and the copper plate attached to the toroidal dewar was assumed to be very large because the interface has a large contact area, a layer of indium foil was used between the niobium and the copper, and the design allows a large contact force to be applied. Thus, the end of the niobium was assumed to be at the same temperature as the copper plate.

Dynamic heat loads could be simulated by applying 45 W of heating into a resistance wire attached to the outer conductor. The measured power coupler dynamic heat loads were about 30 W in the upper temperature hex (operating at 20 K), about 10 W in the lower temperature hex (operating at 8 K), and 1.4 W going to 4 K. The measured static loads appear to be about 12 W, 2.5 W, and 1.1 W in the high and low temperature hex's and into 4 K respectively. Generally, the thermal model predicted 4 K heat loads that were 1/2 to 1/4 of that measured. The predicted heat loads at the thermal intercepts were typically less than the measured values but never by more than 25%.

SENSITIVITY ANALYSIS

The thermal model is a powerful tool in evaluating the sensitivity of heat load to almost any parameter. Each model run takes less than one minute. Thus, the model is also very efficient in evaluating sensitivities. The time consuming effort is in handling the non-linearity of the response of the model. For example, changing the RRR of the copper plated film will change the heat being conducted down the outer conductor, which will impact the performance of the heat exchangers. In the SINDA model, the effectiveness of the heat exchangers is assumed to be constant. The hex's are modeled explicitly in a separate thermal analysis based on calculating the Reynold's number, then the Nusselt number, the heat transfer coefficient, etc., but, there are irregularities in performance that cannot be explained. There is insufficient space in this article to discuss this issue further, but for more information, see [13].

An abbreviated sensitivity analysis was performed. The effectiveness of the high and low temperature thermal intercept heat exchangers were kept constant at 0.9 and 0.6. The coolant mass flow rate was kept constant at 0.4 g/s. The RF simulated 45 W was implemented. The heat load to 4 K was considered the most important output parameter and it is largely controlled by the properties of the spool piece and its thermal intercepts and the Nb nipple. Hence, only factors associated with those components were varied.

Not surprisingly, the results indicate that the strongest influence on the 4 K heat load is from the wall temperature at the two thermal intercepts. Decreasing the upper (lower) temperature hex wall temperature by 9% (4%) lowered the 4 K heat load by 18% (6.5%). Increasing the emissivities of the SS, Nb, and Cu from 0.08, 0.1, and 0.05 to 0.3, 0.3, and 0.1 respectively, increased the 4 K heat load by 40% indicating the need for manufacturing attention to detail in the plating, handling and assembly operations.

THERMAL OSCILLATIONS

During the experiments in the CTR, oscillations were observed in the inlet, outlet, and wall temperatures of the thermal intercept heat exchangers. Oscillations were also observed in the pressure and mass flow rates of the coolant. Figure 5 is representative of some of the extensive data taken. The amplitudes of the various oscillating parameters varied from experiment to experiment and sometimes diminished to zero over time and sometimes spontaneously started after the system seemed to have reached a steady state.

Oscillations with two periods were observed. One series had a period of about 240 seconds and probably corresponds to thermal density wave oscillations [11]. The period corresponds to the transit time, at the speed of sound, through the coolant loop from the liquefier, through the 4000 L dewar, into the CTR, through the outer conductor hex's, and finally to the flow control needle valve at room temperature.

The other oscillations had a period of about 0.3 seconds. These appear too slow for thermal acoustic oscillations and too fast for thermal density waves. All attempts to link these oscillations to the refrigerator, expansion engines, compressors, or other parts of the coolant flow system were unsuccessful. Additional studies and experiments are needed.

SUMMARY

The Cryogenic Test Rig (CTR) was built to measure the heat leaks from the APT power coupler. Measurements of temperature and heat leaks were used to validate a

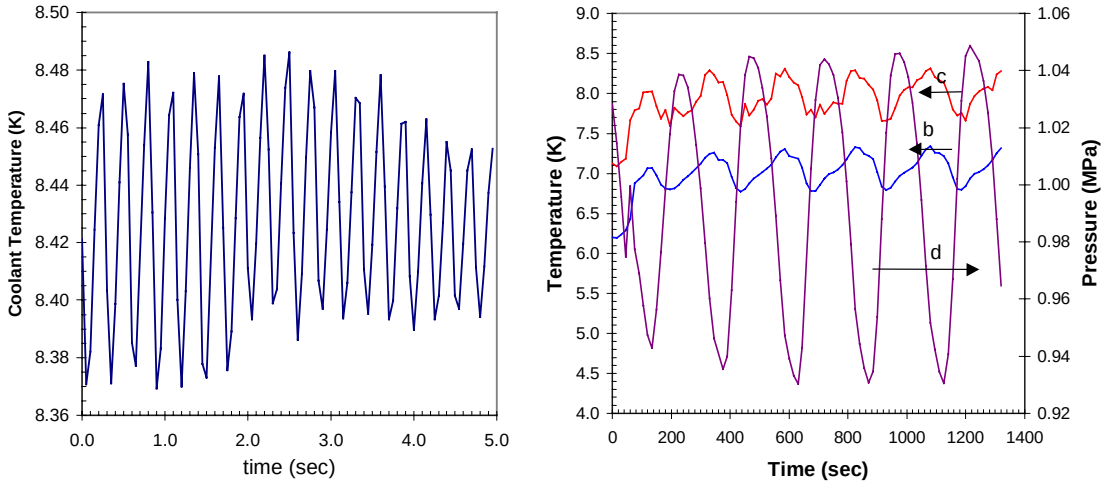

FIGURE 5. Plots showing an example of thermal oscillations observed during the CTR experiments. Graph on the left is the wall temperature of the low temperature hex; the period is about 0.26 sec. The graph on the right shows the helium coolant pressure (curve d) and the inlet (b) and outlet (c) temperatures of the low temperature hex.

thermal model. The CTR performed adequately, especially considering that some of the ancillary equipment such as the model 1610 helium liquefier was not intended for this purpose. The experimental data and model predictions agree quite well. With reasonable adjustments to the input parameters, the temperature distributions predicted by the thermal model agree well with the thermal measurements, usually within a few percent. The heat leak to 4 K, as measured, is typically 50% larger than that predicted by the model. This level of discrepancy is not unusual for low temperature cryogenic measurements, especially at these relatively low heat leaks (less than 2 W) measured on large components such as the power coupler.

REFERENCES

1. Waynert, J.A., Prenger, F.C., and Kelley, J.P., "Thermal Optimization of the APT Cryomodule with Regard to the Associated Cryosystem," in *Advances in Cryogenic Engineering* **45A**, edited by Quan-Sheng Shu et al, Plenum, New York, 1999, pp.947-952.
2. Waynert, J. A. and Prenger, F. C., "A Thermal Analysis and Optimization of the APT 210 kW Power Coupler," LINAC98 Proceedings (1998).
3. RadCAD, CAD based thermal radiation analyzer, Cullimore and Ring Technologies, Inc., Littleton, CO.
4. SINDA, Systems Improved Numerical Differencing Analyser, Cullimore and Ring Technologies, Inc., Littleton, CO.
5. MAFIA, Electromagnetic Siulator, CST, D-64289 Darmstadt, Germany.
6. Helium property data was taken from HePak by Cryodata, Inc., Louisville, CO.
7. Van Sciver, S.W., Nilles, M.J., and Pfotenhauer, J., "Thermal and Electrical Contact Conductance between Metals at Low Temperatures," Proc. Of Space Cryogenics Workshop **36**, 1984.
8. Salerno, L.J., Kittel, P., Spivak, A.L., *AIAA Journal* **22**, pp. 1810-1816 (1984).
9. Waynert, J.A. LANL ESA-EPE Memo: 00-049, *Initial Power Coupler Heat Leak Measurements in the CTR and a Comparison to Thermal Model Predictions*, Jan. 2000.
10. Gubareff, G.G., Janssen, J.E., and Torborg, R.H., *Thermal Radiation Properties Survey*, Honeywell Research Center, Minneapolis, MN 1960.
11. *Table of Emissivity of Various Surfaces for Infrared Thermometry*, Micron Instrument Co., Wyckoff, NJ.
12. Reed, R.P., and Clark, A.F., *Materials at Low Temperatures*, American Society of Metals, Metals Park, OH 1983, p.152.
13. Waynert, J.A. LANL ESA-EPE Memo: 01-012, *Final Results: Power Coupler Thermal Measurements From CTR Compared to Model Predictions*, Nov. 2001.
14. Daney, D.E., Ludtke, P.R., and Jones, M.C, *ASME J. Heat Transfer* **101**, pp. 9-14 (1979).